

# Application of MAT Device to Characterize the Adhesive Bonding Strength of Membrane in Orthotropic Steel Deck Bridges

X.Liu , A. Scarpas, J. Li, G. Tzimiris

(Delft University of Technology, Stevinweg 1, 2628 CN Delft, the Netherlands, X.Liu@tudelft.nl)

## ABSTRACT

In order to characterize adequately the adhesive bonding strength of the various membranes with surrounding materials on orthotropic steel decks and collect the necessary parameters for FE modeling, details of the Membrane Adhesion Test (MAT) have been introduced. Analytical constitutive relations of MAT device have been derived on the basis of Williams (1997). Furthermore, on the basis of experimental data obtained from MAT, ranking of the bonding characteristics of various membrane products is demonstrated as well as the role of other influencing factors, such as the types of substrate and test temperatures.

**Keywords:** Membrane; Orthotropic steel deck bridge; Adhesive bonding strength; Finite element; Strain energy release rate.

## 1. INTRODUCTION

The world-wide reported distress problems between the surfacing layers and the decks of orthotropic steel bridges indicate the need for further research on the interaction between them. The severity of the problem is enhanced by the considerable increase in traffic in terms of number of trucks and heavier wheel loads. Innovative methodologies offer opportunities to mitigate material response degradation and fatigue related problems in this type of structures contributing thus to significant extension of the service life of steel bridges.

Preliminary investigations [1][2] have shown that the adhesive strength of membrane layer between the surfacing layers and the decks of steel bridges has a strong influence on the structural response of orthotropic steel bridge decks. The most important requirement for the application of membrane materials on orthotropic steel bridge decks is that the membrane adhesive layer shall be able to provide sufficient bond to the surrounding materials.

A number of techniques have been developed in the past to quantify the adhesive strength between membrane and the associated substrate. Among others, the blister tests, initially suggested by Dannenberg (1958) [3] and discussed by Gent and Lewandowski (1987) [4], is the most common used one. The test specimen in the blister test consists of a perforated substrate with a thin flexible bonded membrane. A fluid is injected at the interface through the perforation, thereby causing a progressive debonding of the membrane. However, blister tests have several drawbacks such as the strain energy release rate increases as blister radius increases and membrane debondings become unstable. The bulged area is anomalous and unpredictable especially when the substrate materials are harsh and porous, for example, cement concrete or porous asphalt concrete. It is vague about the physical or chemical effects of the pressurized liquid on interface between the two bonded materials.

Shaft loaded blister test (SLBT), first proposed by Williams (1969) [5], is an alternative to the pressured blister test. A machine driven shaft is utilized to induce central loads and displacements on membrane. Because of the slightly simpler setup and loading method, SLBT has its advantages over traditional blister test and received much attention in the last two decades. The main limitation of the SLBT is about the stress singularity caused by its shaft point load. Different kinds of shaft cap shapes are employed to improve this weakness. Most common way is using a spherically capped shaft or ball with certain radius, [6] and [7].

Peel test is also the most commonly used to quantify the adhesive strength of membrane to the associated substrate. However the peel test usually causes large permanent deformation at the loading point, which makes the calculation of energy release rate inaccurate. The majority of

mechanical energy supplied in peeling is dissipated or stored in deforming the test specimen and relatively little energy actually contributes to the fracture process of the interface

In the recent years, considerable number of analytical solutions for blister tests, SLBT and peel tests are deducted. The representative contributions include [8], [5], [9], [10] and [11].

In order to characterize adequately the adhesive bonding strength of the various membranes with surrounding materials on orthotropic steel decks and collect the necessary parameters for FE modeling, a Membrane Adhesion Test (MAT) device has been developed by Delft University of Technology. The innovative MAT device has the several advantages. Due to utilize of cylindrical loading piston head, the piston force can be applied uniformly on the membrane surface with small boundary effect. The cylindrical loading piston heads designed with different radius are optional to minimize damage on the test membrane so that the reliability of test results is guaranteed. The relatively simple analytical solution of the constitutive relation, the energy release rate and membrane strain expressions can be derived. A laser scanning system is utilized to measure membrane deformation, hence the in time membrane deformed profile can be recorded.

In this paper, details of the MAT test have been introduced to characterize the adhesive characteristics of the various membranes with the surrounding materials. Analytical constitutive relations of MAT device have been derived on the basis of Williams (1997) [10]. Furthermore, on the basis of experimental data obtained from MAT device, ranking of the bonding characteristics of different membrane product is demonstrated as well as the role of other influencing factors, such as the substrate type and test temperature. Availability of the MAT results will allow a better understanding of performance of the membrane allowing thus optimization of maintenance activities.

## 2. APPARATUS

The MAT test system consists of a loading device, an environmental chamber, laser scanning device and a data acquisition system. The loading device includes a computer controlled loading component which, during each loading cycle, in response to commands from the data processing and control component, adjusts and applies a load on the tested membrane. The loading device is capable of (1) providing repeated haversine loading at a frequency range of 0 Hz to 12 Hz, (2) rising the piston to the maximum distance 130 mm after the piston is in contact with the test membrane, (3) providing a maximum force up to 5 kN, (4) providing two piston heads with radius of 90 mm and 75 mm. Fig. 1 illustrates the components of the MAT device.

The laser scanning system senses the shape of the deformed object and collects data that defines the location of the outer surface of the membrane. A line laser is utilized to measure the membrane in time deformed profile across 150 mm width. The laser scanner can be operated in temperature range of  $-10^{\circ}\text{C}$  to  $55^{\circ}\text{C}$ . The frequency of the laser scanner is up to 250Hz for the full range.

An environmental chamber is utilized to enclose the entire test set up and maintains the specimen at controlled temperature. The environmental chamber is not required if the temperature of the surrounding environment can be maintained within the specific limits. The chamber can provide temperature range of  $-15^{\circ}\text{C}$  to  $80^{\circ}\text{C}$  and relative humidity range of 10% to 95%.

During each load cycle the control and data acquisition system are capable of measuring the load and deformation of the piston and adjusting the load or displacement applied by the loading device and the loading frequency. In addition, it is capable of recording load cycles, applied loads, and piston deformations.

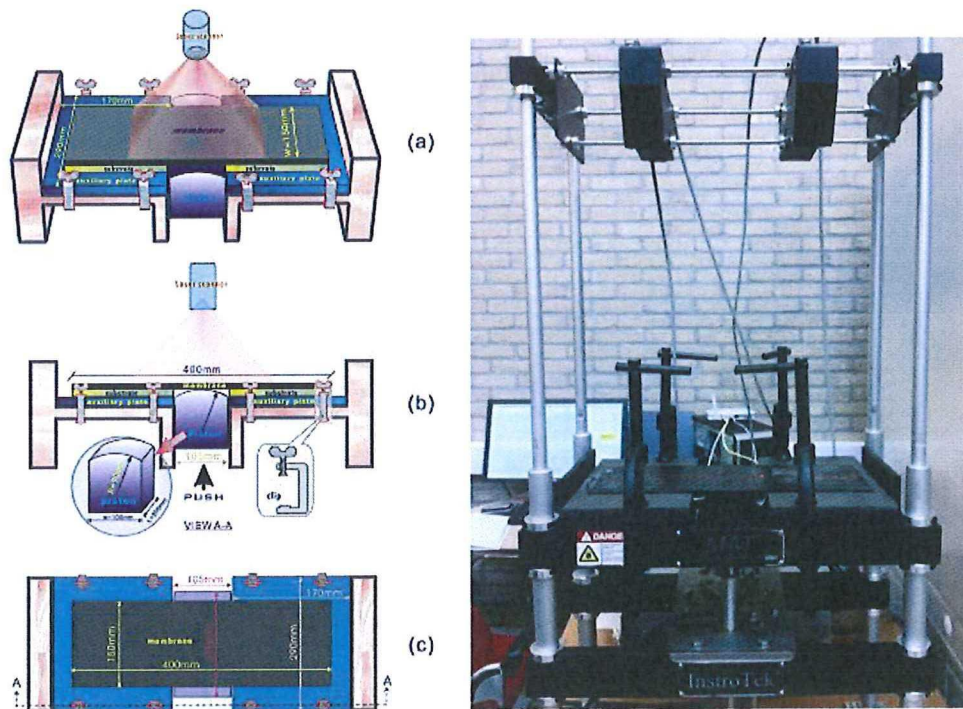


Figure 1 Schematic of MAT device

### 3. SPECIMEN PREPARATION

In the Netherlands an asphaltic surfacing structure for orthotropic steel bridge decks mostly consists of two structural layers. The upper layer consists of Porous Asphalt (PA) because of reasons related to noise hindrance. For the lower layer a choice between Mastic Asphalt (MA) or Guss Asphalt (GA), can be made, see Figure 2. In order to characterize the adhesive bonding strength of various membrane products utilized in the Dutch steel deck bridges, three types of specimen, i.e. steel-membrane specimen (SM), Guss Asphalt Concrete-membrane specimen (GM) and Porous Asphalt-membrane specimen (PM), are included in this research project, see Figure 3.

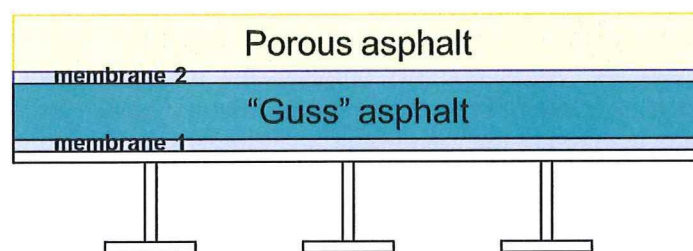


Figure 2 Schematic of a typical Dutch asphalt surfacing system on a steel bridge desk

For the SM specimen preparation, two pieces of square steel plates with thickness 6 mm is used. The steel plate shall be cleaned in accordance with EN ISO 8503-1. The membrane with dimension  $t$  is the thickness of the tested membrane shall be bonded to the steel plate in accordance with standard procedures provided by membrane manufacturers.

Because the GM system consists of two interfaces, one is the membrane on the bottom of the guss asphalt (named GM1) and another is the membrane on the top of the guss asphalt (named GM2). Therefore two types of GM specimens shall be prepared. Due to the physical characteristics of Guss asphalt, a mould shall be utilized for preparation of GM specimens. The procedures of installation of membrane on top or bottom of the guss asphalt shall be according to the membrane manufacture specification.

For the preparation of PM specimen, a mould is utilized. The PM specimen dimension is 400mm by 150mm by 40mm. The porous asphalt is compacted on top of the membrane. After compaction, the porous asphalt requires a minimum curing time of 14 days and a maximum of 8 weeks before testing. Porous asphalt preparation shall be performed in accordance with NEN-EN 12697-33.

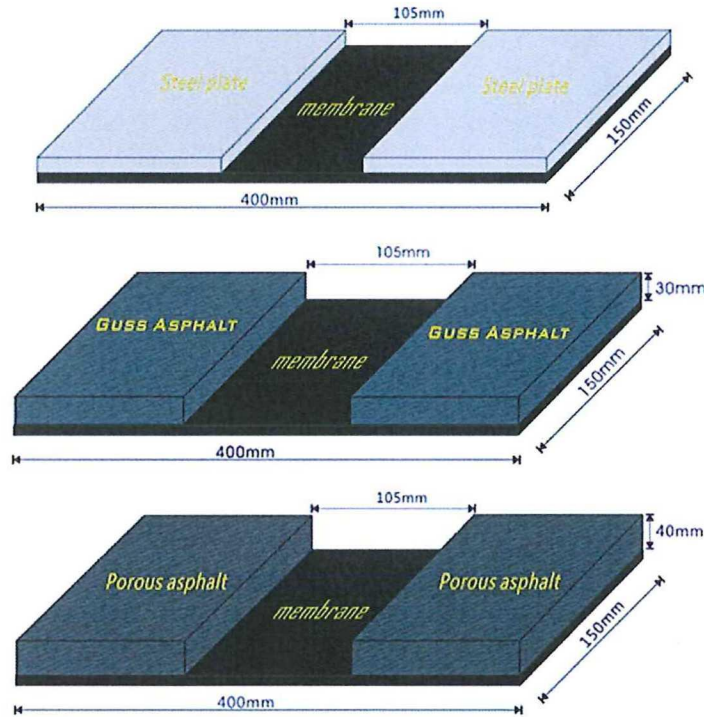


Figure 3 Schematic of the MAT specimens

#### 4. CONSTITUTIVE RELATIONS

In order to derive the constitutive relations of MAT test, a deformed thin membrane with thickness  $h$  and width  $b$  is shown in Figure 4. A central load  $F$  is applied to the membrane via a cylindrically capped piston with radius  $R$ . The deformed height of the centre point at the outer surface of the membrane is  $H$ . There are two contact situations that may occur in the MAT tests. The first situation is that the piston partially contacts the membrane, see Figure 4. The second situation is the membrane contacts fully to the piston and the membrane will be stretched in straight after the kinks of the piston touch to the membrane, see Figure 5.

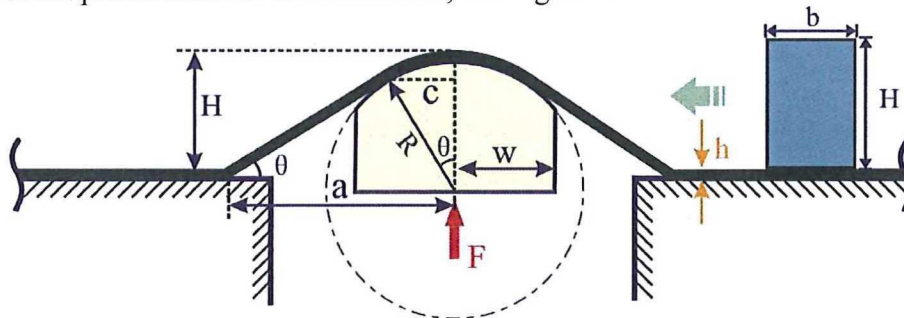


Figure 4 Cylindrically capped MAT (membrane contacts partially to the piston head)

The complete solutions of the load point height  $H$  and the membrane strain are summarized by the combinations of the aforementioned two contact situations:

$$H = \begin{cases} a \tan \theta - R \left( \frac{1 - \cos \theta}{\cos \theta} \right) & \left( \sin \theta \leq \frac{W}{R} \right) \\ (a - W) \tan \theta + R - \sqrt{R^2 - W^2} & \left( \sin \theta > \frac{W}{R} \right) \end{cases} \quad (1.1)$$

$$\varepsilon = \begin{cases} \left( \frac{1 - \cos \theta}{\cos \theta} \right) + \frac{R}{a} (\theta - \tan \theta) & \left( \sin \theta \leq \frac{W}{R} \right) \\ \left( \frac{1 - \cos \theta}{\cos \theta} \right) - \frac{W}{a \cos \theta} + \frac{R \theta_0}{a} & \left( \sin \theta > \frac{W}{R} \right) \end{cases} \quad (1.2)$$

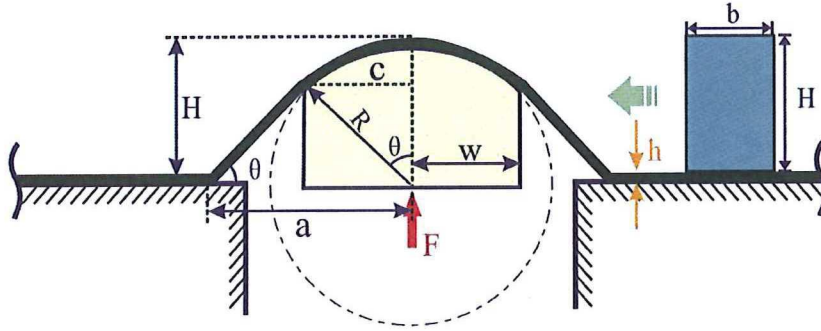


Figure 5 Cylindrically capped MAT (membrane contacts fully to the piston head)

In order to derive the relationship between actuator load  $F$  and the membrane strip angle  $\theta$ , a schematic of force resolution for MAT is illustrated in Figure 6.

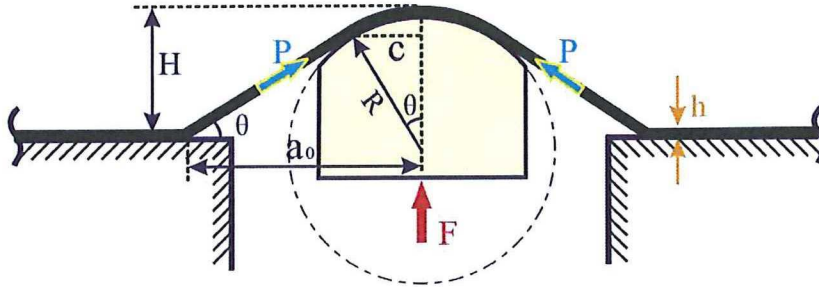


Figure 6 Force resolution for MAT

Force along membrane strip is:

$$P = \frac{F}{2 \sin \theta} = \sigma b h \quad (1.3)$$

Actuator load  $F$  becomes:

$$F = 2 \sigma b h \sin \theta \quad (1.4)$$

Furthermore, for elastic membrane, the actuator load for the aforementioned two contact situations can be expressed by:

$$F = 2 b h \sigma \sin \theta = \begin{cases} 2 b h \sin \theta E \left[ \left( \frac{1 - \cos \theta}{\cos \theta} \right) - \frac{R}{a} (\tan \theta - \theta) \right] & \left( \sin \theta \leq \frac{W}{R} \right) \\ 2 b h \sin \theta E \left[ \left( \frac{1 - \cos \theta}{\cos \theta} \right) - \frac{W}{a \cos \theta} + \frac{R \theta_0}{a} \right] & \left( \sin \theta > \frac{W}{R} \right) \end{cases} \quad (1.5)$$

## 5. STRAIN ENERGY RELEASE RATE

The strain energy release rate  $G$  characterizes the energy per unit crack or debonding area required to extend, and as such is expected to be the fundamental physical quantity controlling the behavior of the material bonding strength. Considering a membrane adhered to a substrate as shown in Figure 4, using a Griffith argument [12], the general definition of energy release rate can be expressed by:

$$G = \frac{d}{dA} [U_{\text{ext}} - U_s - U_d - U_k] \quad (1.6)$$

where  $U_{\text{ext}}$  is the external work;  $U_s$  is the strain energy;  $U_d$  is the dissipated energy;  $U_k$  is the kinetic energy;  $A$  is the area create.

By considering a strip membrane bonded to a substrate surface and debonded over a length  $2a$  in Figure 7,  $H$ ,  $a$  and  $\theta$  change during membrane debonding but with the continuity condition the slopping length  $2s$  is increased such that  $ds = da$ . Now that  $a = s \cdot \cos\theta$  and  $H = s \cdot \sin\theta$ , i.e.

$$\frac{da}{d\theta} = \frac{ds}{d\theta} \cdot \cos\theta - s \cdot \sin\theta = -\frac{s \sin\theta}{1 - \cos\theta} \quad (1.7)$$

also

$$\frac{dH}{d\theta} = \frac{ds}{d\theta} \cdot \sin\theta + s \cdot \cos\theta = -s \quad (1.8)$$

hence

$$\frac{dH}{da} = \frac{1 - \cos\theta}{\sin\theta} \quad (1.9)$$

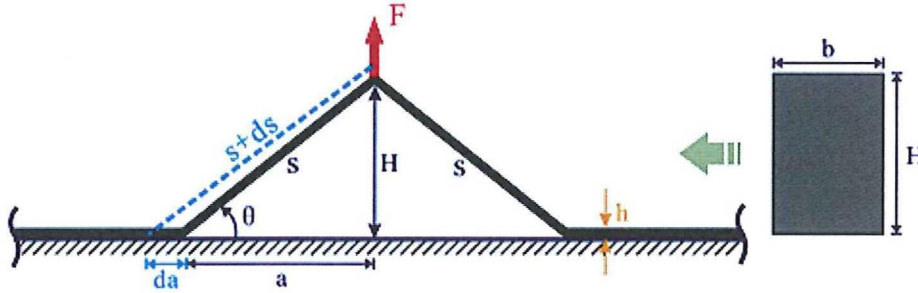


Figure 7 Schematic of debonded membrane strip

According to Williams (1997) [10], for a flexible but inextensible membrane strip with a slow peeling load, the strain energy release rate becomes:

$$G = \frac{dU_{\text{ext}}}{2bda} = \frac{F \cdot dH}{2bda} = \frac{F}{2b \sin\theta} (1 - \cos\theta) \quad (1.10)$$

For linear elastic and extensible membrane strip in Figure 7, the energy release rate in Eq. (1.10) can be written by:

$$G = \frac{F}{2b \sin\theta} \left( 1 - \cos\theta + \frac{\varepsilon}{2} \right) \quad (1.11)$$

By substituting Eq. (1.2) into(1.11), the strain energy release rate  $G$  of MAT test becomes:

$$G = \begin{cases} \frac{F(a \cos \theta - 2a \cos^2 \theta + a + R\theta \cos \theta - R \sin \theta)}{4ab \sin \theta \cos \theta} & \left( \sin \theta \leq \frac{W}{R} \right) \\ \frac{F(a \cos \theta - 2a \cos^2 \theta + a + R\theta_0 \cos \theta - W)}{4ab \sin \theta \cos \theta} & \left( \sin \theta > \frac{W}{R} \right) \end{cases} \quad (1.12)$$

Since the actuator load  $F$  and membrane strip angle  $\theta$  in Eq. (1.12) can be measured directly via MAT device, the critical value of  $G=G_c$  can be determined when the membrane starts to debond.

## 6. RESULTS AND DISCUSSIONS

In this paper, MAT monotonic test results of three different membranes indicated by AA, BB and CC bonded with three different substrates (Steel, Guss asphalt and Porous asphalt) are presented. To determine the role of ambient temperature, the tests were performed over the range of temperatures ( $-5^\circ\text{C}$ ,  $+5^\circ\text{C}$  and  $+10^\circ\text{C}$ ).

Figure 8 through Figure 11 show the variations of piston reaction force obtained by MAT device versus the membrane debonding length. The following observations are made:

- The mechanical response of membrane product is influenced not only by the surrounding substrate but also by the environment temperature;
- Initially the piston reaction force increases linearly. In most cases there is either a gradually increasing nonlinearity or sudden crack extension and arrest (called ‘pop-in’) followed by nonlinearity;
- In most cases, product BB shows a higher reaction force development than the product AA and CC;
- All products within SM, GM1 and PM samples show a higher reaction force at lower temperature except the one within GM2 samples;

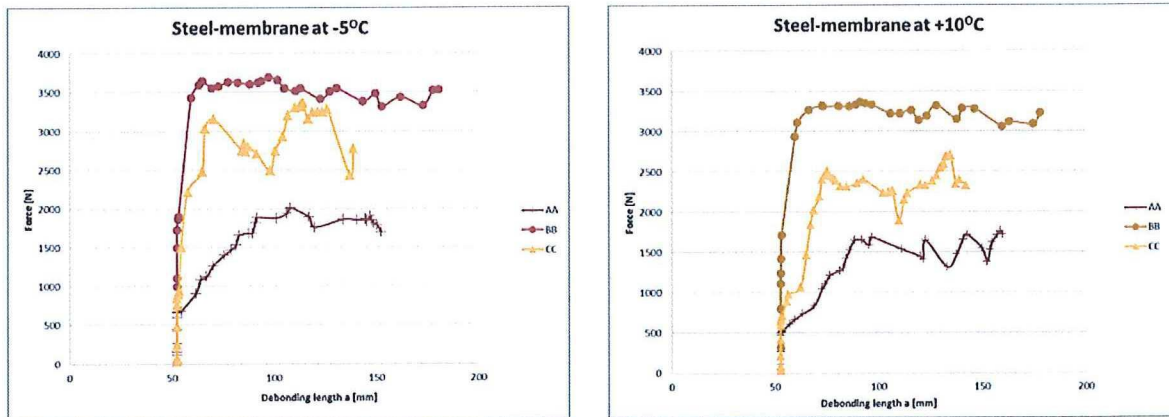


Figure 8 Force versus debonded length of SM samples

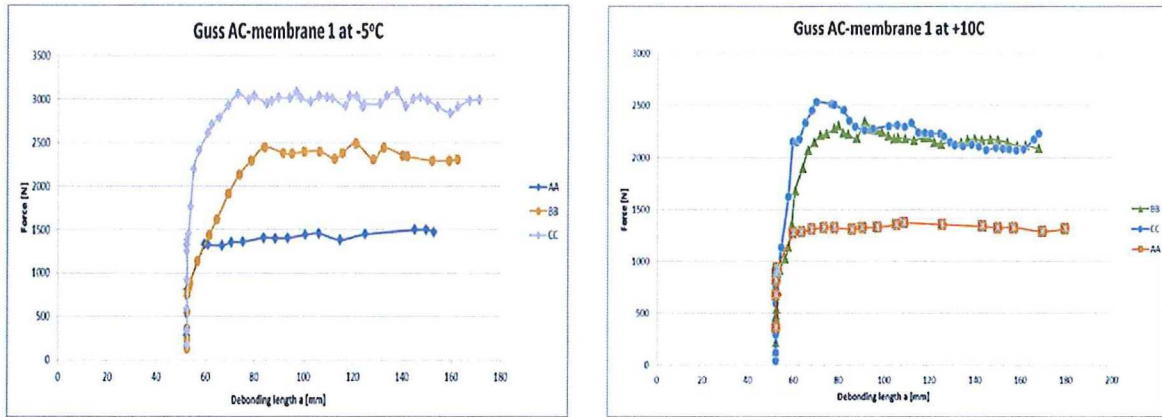


Figure 9 Force versus debonded length of GM1 samples

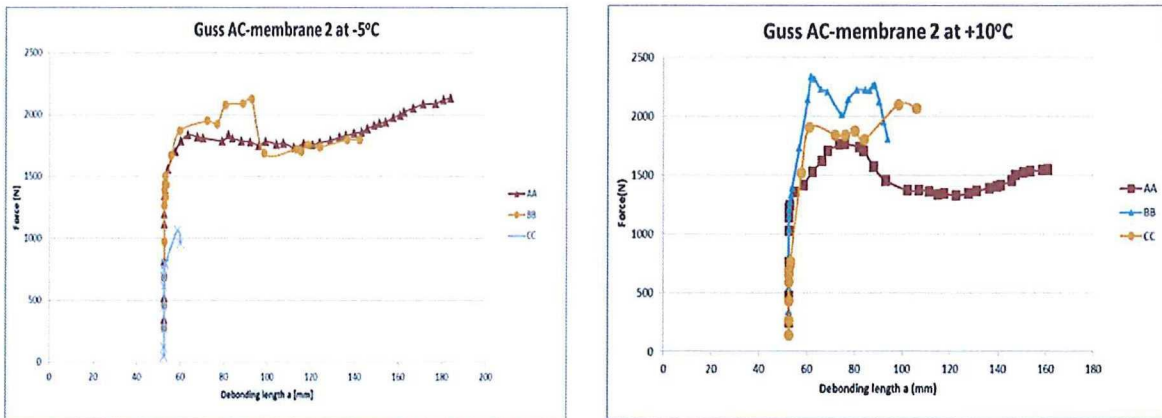


Figure 10 Force versus debonded length of GM2 samples

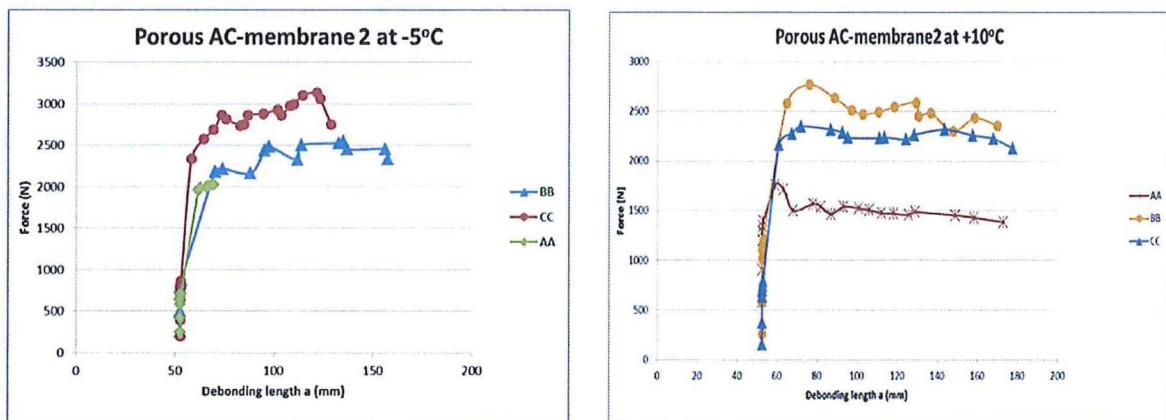


Figure 11 Force versus debonded length of PM2 samples

Figure 12 gives the comparison of critical strain energy release rate  $G_c$  among different samples over the range of temperatures ( $-5^{\circ}\text{C}$ ,  $+5^{\circ}\text{C}$  and  $+10^{\circ}\text{C}$ ). The following observations and conclusions are made

- The bonding strength of membrane products depends on both the characteristic of substrate material and the environment temperature;
- In general, product BB with GM and PM samples gives higher  $G_c$  at all test temperatures. Product AA and CC with PA samples show  $G_c$  values decreasing when temperature is increased. Product CC with SM and GM2 samples shows  $G_c$  values increasing when temperature is increased; Products AA, BB and CC with GM1 samples show a higher  $G_c$  at  $+5^{\circ}\text{C}$ ;



- By comparing Figure 12 with Figure 8 through Figure 11, it can be observed that higher maximum piston reaction force does not necessarily result the higher  $G_c$  values. These inconsistency may occur due to that piston maximum reaction force represents both membrane material response and membrane bonding characteristics. However  $G_c$  is a material physical quantity controlling the behavior of only the membrane bonding strength;

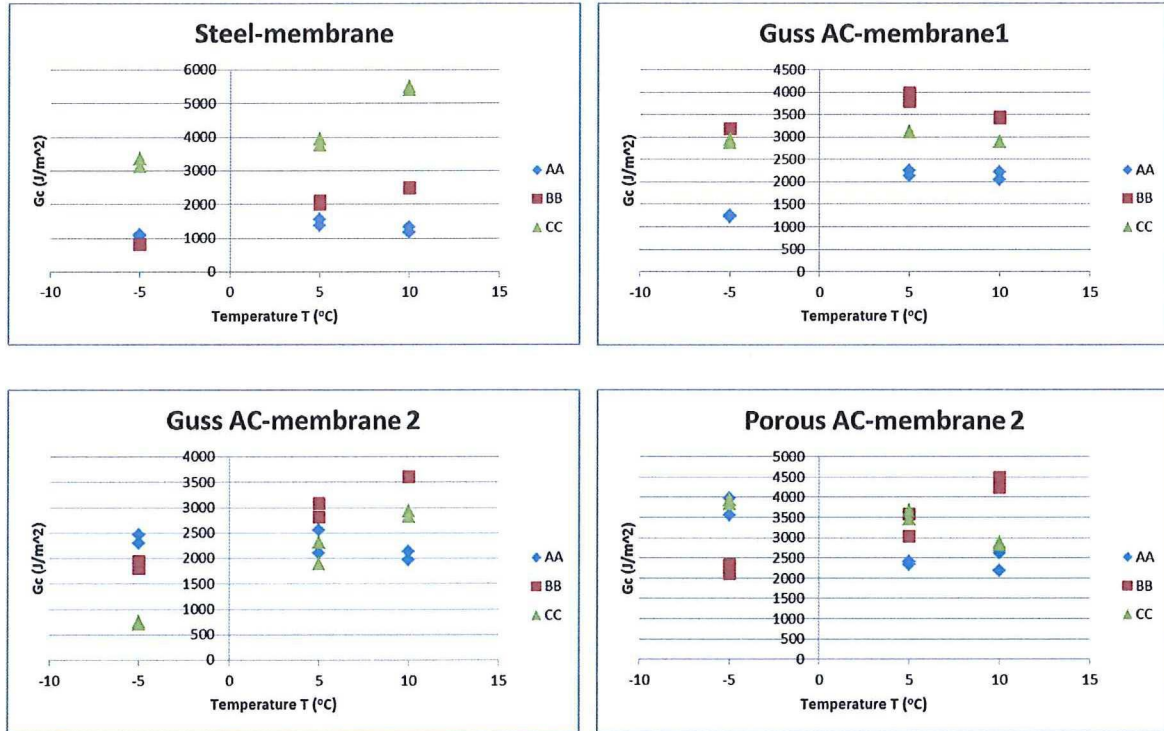


Figure 12 Comparison of strain energy release rate among different samples

## 7. CONCLUSIONS AND RECOMMENDATIONS

Based on the results presented in this paper, the following conclusions and recommendations can be made.

- The MAT setup is capable of characterizing the adhesive bonding strength of the various membranes with the surrounding materials. MAT results will allow a better understanding of performance of the membrane on the bridge structure allowing thus optimization of maintenance activities;
- Critical strain energy release rate  $G_c$  is a fundamental physical quantity that can be utilized to quantify the membrane adhesive bonding strength with different substrates;
- The bonding strength of membrane product depends both on the characteristic of substrate material and the environment temperature;
- In the near future, the MAT cyclic load test will be developed to characterize the membrane fatigue life. The influence of the material nonlinearity on membrane adhesive strength and fatigue life shall be further studied .

## ACKNOWLEDGMENT

This research project is funded by the Dutch Transport Research Centre (DVS) of the Ministry of Transport, Public Works and Water Management (RWS). Their financial support is highly

appreciated. We would like to sincerely thank Miss YanYang for her contribution to the data post-processing.

## REFERENCES

- [1]Liu, X., Medani, T. O., Scarpas, A., Huurman, M. and Molenaar, A. A. A."Experimental and numerical characterization of a membrane material for orthotropic steel deck bridges: Part 2 - Development and implementation of a nonlinear constitutive model," *Finite Elements in Analysis and Design*, vol. 44, 580-594, 2008.
- [2]Medani, T. O. "Design principles of surfacings on orthotropic steel bridge decks," PhD, Delft University of Technology, Delft, 2006.
- [4]Dannenbergh, H. "Measurement of Adhesion by a Blister Method," *J. Appl. Polym. Sci.*, vol. 33, 509-510, 1958.
- [5]Gent, A. and Lewandowski, L. "Blow-Off Pressures for Adhering Layers," *J. Appl. Polym. Sci.*, vol 33, 1567 -1577(1987).
- [6]Liao, K. & Wan, K. T. "Evaluation of film-substrate interface durability using a shaft-loaded blister test," *J Compos Tech Res*, vol. 23, 15-20, 2001.
- [7]Xu, X. J., Shearwood, C. & Liao, K. "A shaft-loaded blister test for elastic response and delamination behavior of thin film-substrate system," *Thin Solid Films* vol.424, 115-119, 2003.
- [8]Malyshev, B.M. & Salganik, R.L. "The strength of adhesive joints using the theory of cracks," *International Journal of Fracture Mechanics*, vol.1, 15, 1965.
- [9]Storakers, B. & Andersson, B. "Nonlinear Plate-Theory Applied to Delamination in Composites," *J Mech Phys Solids*, vol.36, 689-718, 1988.
- [10]Williams, J. G. "Energy release rates for the peeling of flexible membranes and the analysis of blister tests," *Int J Fracture* vol.87, 265-288, 1997.
- [11]Jin, C. "Analysis of energy release rate and bending-to-stretching behavior in the shaft-loaded blister test," *Int J Solids Struct* vol.45, 6485-6500, 2008.
- [12]Kanninen, M. F. & Poplar, C. H. "Advanced Fracture Mechanics", Oxford University Press, Chapter 3, 1985.